Received: 23 November 2017 | Accepted: 12 February 2018

DOI: 10.1111/gcb.14139

PRIMARY RESEARCH ARTICLE

WILEY Global Change Biology

Elevated CO_2 did not affect the hydrological balance of a mature native *Eucalyptus* woodland

Teresa E. Gimeno[1,2] | Tim R. McVicar[3,4] | Anthony P. O'Grady[5] | David T. Tissue[2] | David S. Ellsworth[2]

[1]INRA, UMR ISPA, Villenave d'Ornon, France

[2]Hawkesbury Institute for the Environment, Western Sydney University, Penrith, NSW, Australia

[3]CSIRO Land and Water, Canberra, ACT, Australia

[4]Australian Research Council Centre of Excellence for Climate System Science, Sydney, NSW, Australia

[5]CSIRO Land and Water, Hobart, TAS, Australia

Correspondence
Teresa E. Gimeno, INRA, UMR ISPA, Villenave d'Ornon, France.
Email: teresa.gimeno@inra.fr

Present address
Teresa E. Gimeno, Basque Centre for Climate Change (BC3), Leioa, Spain.

Funding information
Australian Commonwealth Government; Western Sydney University (WSU) and Australian Commonwealth Scientific and Industrial Research Organisation (CSIRO) Flagship program 'Water for a Healthy Country'; Université de Bordeaux IdEx program and EU H2020 Marie Skłodowska-Curie actions, Grant/Award Number: 653223

Abstract

Elevated atmospheric CO_2 concentration (eC_a) might reduce forest water-use, due to decreased transpiration, following partial stomatal closure, thus enhancing water-use efficiency and productivity at low water availability. If evapotranspiration (E_t) is reduced, it may subsequently increase soil water storage (ΔS) or surface runoff (R) and drainage (D_g), although these could be offset or even reversed by changes in vegetation structure, mainly increased leaf area index (L). To understand the effect of eC_a in a water-limited ecosystem, we tested whether 2 years of eC_a (~40% increase) affected the hydrological partitioning in a mature water-limited *Eucalyptus* woodland exposed to Free-Air CO_2 Enrichment (FACE). This timeframe allowed us to evaluate whether physiological effects of eC_a reduced stand water-use irrespective of L, which was unaffected by eC_a in this timeframe. We hypothesized that eC_a would reduce tree-canopy transpiration (E_{tree}), but excess water from reduced E_{tree} would be lost via increased soil evaporation and understory transpiration (E_{floor}) with no increase in ΔS, R or D_g. We computed E_t, ΔS, R and D_g from measurements of sapflow velocity, L, soil water content (θ), understory micrometeorology, throughfall and stemflow. We found that eC_a did not affect E_{tree}, E_{floor}, ΔS or θ at any depth (to 4.5 m) over the experimental period. We closed the water balance for dry seasons with no differences in the partitioning to R and D_g between C_a levels. Soil temperature and θ were the main drivers of E_{floor} while vapour pressure deficit-controlled E_{tree}, though eC_a did not significantly affect any of these relationships. Our results suggest that in the short-term, eC_a does not significantly affect ecosystem water-use at this site. We conclude that water-savings under eC_a mediated by either direct effects on plant transpiration or by indirect effects via changes in L or soil moisture availability are unlikely in water-limited mature eucalypt woodlands.

KEYWORDS
climate change, *Eucalyptus tereticornis*, free-air CO_2 enrichment, interception, stomatal conductance, tree water, water-use efficiency

1 | INTRODUCTION

Rising atmospheric CO_2 concentration (C_a) directly affects several facets of plant physiology, with cascading effects on other biotic and abiotic ecosystem components (Field, Jackson, & Mooney, 1995). At the leaf-level, increases in C_a above the present concentration often enhance photosynthesis, reduce transpiration, due to partially reduced stomatal conductance (g_s) and thus increase water-use efficiency (De Kauwe et al., 2013; Keenan et al., 2013), though the ecosystem-level ramifications of these effects are still debated

(Donohue, Roderick, McVicar, & Yang, 2017; Leuzinger & Körner, 2010). In vegetated areas, evapotranspiration is a major contributor to ecosystem water balance (Zhang et al., 2016). At steady-state conditions, reduced transpiration under elevated C_a (eC_a) may lead to increased soil moisture (Leuzinger & Körner, 2007) and eventually an increase in the amount of precipitation running off the ground surface (R) and into groundwater stores (D_g, Gedney et al., 2006; Zhang, Dawes, & Walker, 2001). Numerous modelling studies and retrospective analyses have ascribed observed increases in R or soil water storage (ΔS) to rising C_a (Aston, 1984; Betts et al., 2007; Jackson, Sala, Paruelo, & Mooney, 1998; Macinnis-Ng, Zeppel, Williams, & Eamus, 2011). Yet, more recent studies highlight that these observations are strongly dependent on the vegetation type and climate (Cheng et al., 2014; Fatichi et al., 2016; Huntington, 2008; Leuzinger & Körner, 2010). However, these predictions rely mostly on retrospective analyses encompassing the increase in C_a from preindustrial to current C_a levels (Betts et al., 2007; Gedney et al., 2006; Ukkola et al., 2016) and these might not necessarily apply to further projected increases in C_a for the 21st century.

Rising C_a also affects transpiration indirectly (Fatichi et al., 2016), as enhanced total or above-ground productivity would require more water to support more tissue produced in eC_a (Ellsworth et al., 2012; Norby et al., 2005). Satellite observations and model predictions indicate that rising C_a partly underlies the recent global increase in woody biomass and greenness (Zhu et al., 2016), particularly in water-limited regions (Donohue, McVicar, & Roderick, 2009). Increased greenness due to present-day CO_2 fertilization results from greater leaf area per unit of ground area (L, Cheng et al., 2017; McCarthy et al., 2007), which increases transpiration surface area per unit of ground area (Macinnis-Ng et al., 2011). Such an effect may offset or even override potential leaf-level reductions in transpiration. Additionally, increased radiative forcing due to climate change would further offset the potential impacts of reduced stomatal conductance under eC_a (Cheng et al., 2014; Ukkola et al., 2016). Indeed, under eC_a, Donohue et al. (2017) predict no effective ecosystem-level water-savings in either water-limited sites, where increased L offsets leaf-level water-savings, or in so-called "energy-limited" sites (cf. Zhang et al., 2001), where little or no change of leaf-level transpiration is expected and where L is already maximized (Yang, Donohue, McVicar, Roderick, & Beck, 2016). Alternatively, in subhumid and semiarid river basins, increased greenness due to eC_a could increase ecosystem-level water-use and reduce streamflow (Trancoso, Larsen, McVicar, Phinn, & Mcalpine, 2017; Ukkola et al., 2016).

In addition to the impact on transpiration, increased L indirectly alters ecosystem water-use by increasing the evaporative losses due to greater partitioning of incoming precipitation into interception (E_i, Kergoat, 1998), although this might not be the case in forests with vertically angled leaves where increased L is unlikely to contribute to greater throughfall (Crockford & Richardson, 2000). Additionally, increased foliage shading decreases the amount of radiation reaching the ground surface, thus decreasing understorey transpiration and soil evaporation (Crockford & Richardson, 2000; Raz-Yaseef, Rotenberg, & Yakir, 2010). Ultimately, the contribution of these later components will be strongly determined by the amount and characteristics of the precipitation events and the dynamics of atmospheric evaporative demand.

Predictions of the impact of eC_a on forest hydrology are largely derived from leaf-level studies (Field et al., 1995; Gimeno et al., 2016), models (Betts et al., 2007) and retrospective analyses (Yang, Donohue, McVicar, Roderick et al., 2016), with additional insights from Free-Air CO_2 Enrichment (FACE) experiments conducted in forests (Donohue et al., 2017). Some of these FACE studies found partial reductions in g_s (Ellsworth, 1999; Gimeno et al., 2016; Gunderson et al., 2002; Keel, Pepin, Leuzinger, & Körner, 2007) and reduced canopy transpiration (Cech, Pepin, & Körner, 2003; Wullschleger & Norby, 2001), while others did not find a reduction in either leaf- or canopy-level transpiration (Uddling, Teclaw, Pregitzer, & Ellsworth, 2009; Ward et al., 2013). In addition, leaf-level water-savings were often offset by increased L (Bobich, Barron-Gafford, Rascher, & Murthy, 2010; Schäfer, Oren, Lai, & Katul, 2002; Tor-ngern et al., 2015; Warren et al., 2011). All of these studies focused mainly on the effect of eC_a on canopy transpiration (E_{tree}), while other components of evapotranspiration (E_t) were rarely measured (Cheng et al., 2017; but see Schäfer et al., 2002). Furthermore, these studies are primarily restricted to energy-limited or moderately water-limited young trees or forest plantations (Bobich et al., 2010; Ellsworth, 1999; Godbold et al., 2014). In water-limited woodlands, we are less likely to observe a change in R or D_g under eC_a, as potential increases in soil moisture could be lost via ground evaporation and understorey transpiration (Ferretti et al., 2003; Nolan, Lane, Benyon, Bradstock, & Mitchell, 2014; Nowak et al., 2004), although this could be partially offset by reduced g_s under eC_a in the understorey (Morgan et al., 2004). Notwithstanding previous work in tree plantations (Schäfer et al., 2002; Uddling et al., 2009; Wullschleger & Norby, 2001), we still lack an experimental test of the effects of eC_a on hydrological partitioning, particularly in mature woodlands experiencing potential water deficits throughout the year. To validate dynamic vegetation models for predicting vegetation–climatic feedbacks, large-scale observations simultaneously addressing the impact of eC_a on all E_t components (not just E_{tree}), R and ΔS are desperately needed (Fisher et al., 2017; Porporato, Daly, & Rodríguez-Iturbe, 2004).

In our study, a mature and water-limited *Eucalyptus* woodland was exposed to a C_a 150 μmol/mol above ambient, using Free-Air CO_2 Enrichment (the "EucFACE" experiment). Here, we address the effects of eC_a on precipitation partitioning among components of the hydrological balance (E_t, R, D_g and ΔS) over the first 2 years of the EucFACE experiment. Duursma et al. (2016) demonstrated that L did not respond to eC_a in this woodland, so we hypothesized (i) that partial stomatal closure at the leaf-level (Gimeno et al., 2016) would lead to a decrease in E_{tree} under eC_a; however, since g_s did not decrease under eC_a in the understorey (Pathare et al., 2017) we expected (ii) that excess water "saved" by the canopy would be lost via increased soil evaporation together with understorey transpiration (E_{floor}), (iii) thus resulting into no net increase in ΔS, R or D_g.

The lack of structural changes induced by eC_a in this timeframe (Duursma et al., 2016), means that we have the advantage that we can carefully examine the partitioning of eC_a effects on water balance components without being confounded by stand structure effects.

2 | MATERIALS AND METHODS

2.1 | Study site and experimental design

EucFACE is located on an ancient alluvial floodplain, 3.6 km from the Hawkesbury River, in western Sydney (NSW, Australia, 33°37′S, 150°44′E, 23 m a.s.l.), in a 270 ha patch of native Cumberland Plain woodland (Figure S1). The site is flat (maximum slope: 0.004°), with the lowest land-surface elevations found near ring 5 (Figure S1). The site is characterized by a humid temperate-subtropical transitional climate with a mean annual temperature of 17°C, with January being the hottest (mean daily maximum 30°C) and July the coldest (mean daily minimum 3.6°C), and a mean annual precipitation (P) of 730 ± 30 mm per year, with February being the wettest month (123 ± 16 mm per month) and July the driest (29 ± 5 mm per month, mean ± SE, 1992–2014, Bureau of Meteorology, station 067105, 5 km away). Satellite-estimated actual E_t is 739 ± 34 mm per year (1981–2012, Zhang et al., 2016), which means that the site is water-limited.

The upper soil (up to 30–50 cm) is a loamy sand (>75% sand), slightly acidic (pH = 4.5) and with low organic C (<1%) and overall low phosphorus (Ellsworth et al., 2017). At 30–70 cm depth, there is a layer of higher clay content (15%–35% clay), below which the soil is a sandy loam or sandy clay loam. Between 300–350 and 450 cm depth, the soil is clay (>40% clay). Groundwater is present at ~12 m below the surface (Figure S2).

Tree density ranges from 600–1000 trees/ha (basal area, BA = 27.6 ± 2.7 m^2/ha, n = 6 plots), L is ≤2 m^2 per m^2 (Duursma et al., 2016), the canopy height is 18–23 m tall and mean tree diameter at 1.3 m (DBH) is 18.8 ± 0.6 cm. The main canopy forming tree is *Eucalyptus tereticornis* Sm. with an understory mainly composed of grasses, with low densities of forbs and occasional shrubs (Pathare et al., 2017).

At EucFACE, there are six 25 m diameter plots (hereafter "rings"). Each ring comprises a cylindrical frame of 28 m high vertical pipes extending above the canopy (treetops ranging 18–23 m). Vegetation within rings 1, 4 and 5 (Figure S1) was exposed to a C_a 150 μmol/mol above ambient, whereas the other three rings received ambient C_a (see Gimeno et al., 2016 for further details). In contrast to previous FACE experiments, here C_a was ramped-up gradually to minimize potential transient effects. Here, the C_a was increased at a rate of ~30 μmol/mol per month over a ~6 month period until C_a reached 150 μmol/mol above ambient in the eC_a rings on the 5 February 2013 (see Drake et al., 2016 for a detailed description of the ramp-up).

2.2 | Meteorological and soil moisture measurements

On top of a central tower (23.5 m) in each ring, an array of sensors measured air temperature and relative humidity (HUMICAP ® HMP 155, Vaisala, Vantaa, Finland), net radiation (R_n, CNR2 Kipp & Zonen, Delf, the Netherlands), photosynthetically active radiation (PAR, LI-190, LI-COR, Inc., Lincoln, NE, USA) and wind speed (Wincap Ultrasonic WMT700 Vaisala, only on the three eC_a rings, Figure S1). These variables were measured every second and 1 (wind) or 10 min (all other variables) averages were recorded on data loggers (CR3000; Campbell Scientific Australia, Townsville, Australia). The average of the six (three for wind) rings was used to characterize the meteorological conditions on site. Daily Penman potential evapotranspiration (E_p) was calculated as (Donohue, McVicar, & Roderick, 2010):

$$E_p = \frac{\Delta}{\Delta+\gamma}R_n + \frac{\gamma}{\Delta+\gamma}\frac{6,430(1+0.536u)D}{\lambda} \quad (1)$$

where γ is the psychrometric constant (65.3 Pa/K), daily R_n integral is in mm per day, D is mean daily water vapour pressure deficit (in Pa), u is mean daily wind speed (in m/s), λ is the latent heat of vapourisation of water (2.45 MJ/kg) and Δ is the rate of change of saturated water vapour with temperature (Pa/K).

Soil volumetric water content (θ_v) was monitored in each ring at eight locations with frequency-domain reflectometers installed at 30 cm depth (TDRs, CS650 Soil Water Content Reflectometer, Campbell Scientific). Soil temperature (T_{soil}) was measured at two locations in each ring with temperature probes at 5 cm depth (TH3-s, UMS GmbH, Frankfurt, Germany). θ_v and T_{soil} were measured every second and 15 min averages were logged on CR3000s.

2.3 | Canopy leaf area measurements

A detailed description of the methods for L (in m^2 per m^2) quantification is found in Duursma et al. (2016). Briefly, L was estimated from diffuse canopy transmittance (τ_d) calculated from the ratio of above- and below-canopy PAR measured in each ring with one and three sensors (LI-190), at 23.5 and 1.5 m height respectively. For these calculations we used only PAR measurements under highly diffuse conditions (diffuse fraction [F_{diff}] > 0.98). We measured F_{diff} with a BF5 Sunshine sensor (Delta-T Instruments, Cambridge, UK) installed on a tower extending 5 m above the canopy at a nearby site (within 2 km). We then calibrated L estimates from τ_d against cumulative litter production over 4 months (Duursma et al., 2016).

2.4 | The water balance components

Mass balance provides a framework for assessing the impact of eC_a on the partitioning of precipitation (P). The mass balance for water can be expressed as:

$$P = R + D_g + \Delta S + E_t \quad (2)$$

where R is surface runoff, D_g is drainage, ΔS is the change in root zone soil-water storage and E_t is evapotranspiration. All variables measured in mm per day. In this study, we assessed the effect of eC_a on E_t and ΔS, while we did not expect a significant effect on R or D_g. Therefore, ΔS, E_t and all of its components were quantified at the ring-level (except for stem-flow, see below) and R and D_g at the site-level. Equation 2 was implemented for 30 months starting on June 2012, including the pretreatment and ramp-up periods.

2.4.1 | Precipitation

We defined a P event as a continuous series of hours with $P > 0$ mm per hr interrupted for 1 hr or less with $P = 0$ mm per hr. Site P was the average of three automated tipping bucket rain gauges (TB4, Hydrological Services Pty Ltd, Liverpool, NSW, Australia) located at the top of the central tower in rings 1, 4 and 3 (Figure S1). P from each bucket was logged every 15 min onto CR3000 data loggers.

2.4.2 | Surface runoff

Surface runoff (R) was calculated as the excess of P minus E_p when the upper soil was saturated and precipitation intensity either exceeded soil infiltration capacity (17 mm per hr for sandy soils, Campbell & Norman, 1998) or cumulative precipitation (P_{cum}) for each event minus E_p exceeded maximum soil storage capacity. In our site, with a sandy soil with $\theta_v = 3\%$ at permanent wilting point and $\theta_v = 30\%$ at saturation and an effective depth of 400 mm, the maximum soil storage capacity was calculated as: $400 \times (30 - 3)/100 = 108$ mm. This approach should be valid for our flat study site with a stratified (or duplex) soil texture with a defined shallow layer of relatively impermeable clay at ~400 mm.

2.4.3 | Drainage and soil water

The D_g from Equation 2 represents the amount of water that drained below the assumed root zone and was not accessible for transpiration. To determine whether the vegetation in our study site was accessing groundwater, we monitored changes of the water table level on-site and analysed the isotopic composition of xylem water and potential water sources (Supporting information). Neither the dynamics of the water table depth (seasonal or intraday), nor the isotopic composition of the tree xylem water suggested that the vegetation at our site used groundwater (Figures S2 and S3).

We assumed that D_g would be water lost from the deep soil layer and calculated D_g as the inverse of the change in soil water storage from 3 to 4.5 m depth. This approach was justified for our site where the soil has a marked multilayered texture: the upper sandy soil (from 0 to 0.3–0.5 m) is where the majority of roots are located (J. Piñeiro et al., *unpublished data*). Below this depth (up to 3 m), the soil is a sandy clay loam (up to 3 m depth) where only a few live roots are present and below 3 m, a clay horizon starts and continues beyond 4.5 m depth. Our observations for root distribution across the depth profile are consistent with the results of Macinnis-Ng et al. (2010) from a nearby (within 7 km) site where ~90% of the tree roots were found in the upper soil (0.7 m) with only occasional roots present in the deeper (up to 1.5 m) clay horizon. We assumed that changes in soil moisture below 3 m are unlikely affected by direct vegetation water uptake or hydraulic lift. Thus, we calculated D_g as water lost below 3 m for a given time interval (t_1-t_2) according to:

$$D_{g,\ t_1-t_2} = -\sum_{i=3}^{z_{max}} \left(\theta_{z_i,t_2} - \theta_{z_i,t_1}\right)\left(z_i - z_{i-1}\right) \quad (3)$$

where θ_{z_i,t_i} is the soil water content at depth z_i and z_{max} is 4.5 m (Duursma et al., 2011). There were no differences in deep soil water storage between ambient and eC_a rings over time ($t = 0.94$, $p = .35$), so D_g was calculated at the site level from averaged deep soil water storage from all rings.

Soil volumetric water content (θ_v) across the soil profile (25–450 cm) was monitored every 15–20 days at two locations in each ring with a neutron probe (NMM, 503DR Hydroprobe®, Instroteck, NC, USA). We measured θ_v in 25 cm intervals from 25 to 150 cm depth and in 50 cm intervals from 150 to 450 cm depth (see Supporting information).

2.4.4 | Change in soil water storage

We calculated the change in soil water storage (ΔS) for a soil column to 3 m depth. Since we expected to observe an effect of eC_a on ΔS, we calculated ΔS for each ring over a given time (t) interval (t_1–t_2) as:

$$\Delta S_{t_1-t_2} = \sum_{i=0}^{z_{max}} \left(\theta_{z_i,t_2} - \theta_{z_i,t_1}\right)\left(z_i - z_{i-1}\right) \quad (4)$$

where θ_{z_i} is the soil water content at depth z_i and z_{max} is 3 m (Duursma et al., 2011). Here, θ_{z_i} is the mean of two measurements at the same depth from two locations within each ring.

2.4.5 | Evapotranspiration

Total ecosystem evapotranspiration (E_t) consists of:

$$E_t = E_i + E_{tree} + E_{floor} \quad (5)$$

where E_i is the canopy interception loss, E_{tree} is overstorey canopy transpiration and E_{floor} is soil evaporation and understorey transpiration.

Interception

Canopy interception loss (E_i) was calculated as:

$$E_i = P - (T_f + S_f) \quad (6)$$

where T_f is throughfall and S_f is stemflow. Throughfall (T_f) was measured under the canopy with one custom-built fixed trough in each ring. Each trough consisted of an 8×0.25 m gutter set with a maximum inclination of 1°. In each ring, T_f was calculated taking into

account the projected area of each gutter. The troughs drained into a large volume tipping bucket flow gauge (TB1L, Hydrological Services Pty Ltd). Total T_f was logged every 15 min onto CR3000 data loggers. One additional trough was located in an open space (Figure S1) to act as a control and we found that this trough underestimated P by 4.4 ± 0.6% (R^2 = .98, p < .001). We assumed that the throughs in the rings underestimated T_f to a similar extent to the control through and corrected accordingly to calculate E_i.

Stem flow (S_f) was measured in 10 trees across EucFACE, adjacent to the study rings, (DBH: 24.6 ± 2.4 cm, range: 14–38 cm). Stem flow collectors were custom-built and consisted of a collar, constructed from a half-split 25 mm diameter vinyl pipe glued with silicone around the trunk. Collectors channelled S_f into automated tipping buckets (TB4) and total S_f was recorded every 15 min onto a CR3000. We used this dataset to model the amount of S_f in each ring. We fitted a linear mixed model to S_f volume collected in each precipitation event as a function of tree basal area, P event size and duration (Crockford & Richardson, 2000), including event as a random factor (Table S1). The obtained coefficients for each fixed factor (tree basal area, P_{cum} and duration) were used to predict S_f of each tree inside each ring, during each precipitation event.

Overstorey canopy transpiration

Whole tree overstorey canopy transpiration (E_{tree}) was computed from measurements of tree sapflow velocity (v_s, Oren, Phillips, Katul, Ewers, & Pataki, 1998). We measured v_s every 10 min using the heat pulse compensation technique (Marshall, 1958) with equipment manufactured by Edwards Industries (Havelock North, New Zealand) and connected to CR3000 data loggers. Each sensor consisted of two temperature probes, constructed of sealed Teflon® 1.8 mm diameter tubing, with each probe containing a negative temperature coefficient thermistor. The temperature sensors were placed 10 mm (downstream) and 5 mm (upstream) from a 1.8 mm diameter stainless steel heater probe. The holes for the temperature and heater probe were drilled with a drill guide to ensure accurate positioning of the probes and parallel alignment. Distances between implanted probes and bark depth were recorded at the time of installation. Measured heat pulse velocity was corrected for the appropriate wound size. The wound width was measured from cut sections of sapwood where "dummy" probes were inserted for 30 days from five trees adjacent to the study plots. Wound size (2.7 ± 0.2 mm) was measured under the light microscope (×40 magnification). v_s was calculated from heat pulse velocity given the fractions of wood and liquid in the sapwood (Swanson & Whitfield, 1981).

In winter 2012, four dominant or codominant trees with positive growth rates for the previous year were selected for monitoring of v_s, in each ring. Two sets of thermocouples and heater element were installed in each tree at 1.3 m height on two randomly selected azimuths. At each tree location, the two thermocouples were positioned at the specific depth below the cambium at which v_s was maximized along the sapwood profile (i.e. both probes in each tree were set at the same depth to get an estimate of within tree radial v_s variability). This depth was determined empirically for each tree as follows: within each tree, one probe was set at 10 mm below the cambium (fixed) and the second probe (mobile) at 25 mm below the cambium. Then, on a cloudless spring day in September 2012, the mobile probe was incrementally pulled out from 25 to 0 mm below the cambium at 5 mm intervals every 90 min (Wullschleger & Norby, 2001). In sensors that were not manipulated, v_s remained relatively constant. With these observations, we determined the depth below the cambium at which v_s was maximal by comparing v_s between the fixed and the mobile probe.

Sapwood area (A_s) and fractions of wood and liquid within the sapwood matrix were calculated from cores extracted from 35 trees adjacent to the study rings. Cores were collected from trees reflecting the size distribution of trees within the rings (DBH: 31.3 ± 2.2 cm). Wood cores were 5 mm in diameter and were extracted using a standard Pressler increment borer (Haglöf Västernorrland, Sweden). Sapwood depth was measured with a digital calliper after staining wood cores with methyl orange that provided visual differentiation of the sapwood from the heartwood (Pfautsch, Macfarlane, Ebdon, & Meder, 2012). We calculated the correlation coefficients between basal area and A_s measured in these trees to predict A_s per unit of ground area from basal area inside each ring.

Mean tree v_s was calculated from the average of the two sets of thermocouples and heater element installed on each tree. We calculated mean hourly v_s for each ring ($\bar{v}_s$) from the four (three in rings 2 and 6) measured trees. Hourly E_{tree} for each ring was calculated as:

$$E_{tree} = \bar{v}_s A_s \quad (7)$$

where A_s is the sapwood area per unit of ground area of each ring. Daily and seasonal water-use per unit ground area for each ring were calculated by integrating E_{tree} over time.

Soil evaporation and understorey transpiration

Soil evaporation together with understorey transpiration (E_{floor}) was estimated from the change in soil moisture over 5 cm depth measured at two locations in each ring with two theta probes (ThetaProbe ML2x, Delta-T). Changes in soil moisture at this depth are likely to reflect E_{floor} because: (i) most understorey vegetation roots are found between 0 and 5 cm depth (J. Piñeiro et al. *unpublished data*); and (ii) changes in soil moisture at this depth are likely to capture water losses due to soil evaporation, given the soil's sandy texture (Campbell & Norman, 1998). Hourly E_{floor} was calculated as:

$$E_{floor,\, t_2-t_1} = z\, \Delta\theta_{t_2-t_1} \quad (8)$$

where z is the depth of the theta probes (5 cm) and $\Delta\theta_{t_2-t_1}$ is the difference in θ_v between consecutive hourly averages (t_1–t_2). A decrease in θ_v from 0 to 5 cm results from evapotranspiration, but also from water infiltration (Schreiner-Mcgraw, Vivoni, Mascaro, & Franz, 2016); thus, to avoid overestimation of E_{floor}, we only calculated E_{floor} for days with P = 0 mm per day and preceded by a day with P < 2 mm per day (454 of 730 days passed these criteria). We validated our approach with E_{floor} measurements made at one location adjacent to ring 1 (Figure S1). An automated long-term clear chamber (LI-8100-104C, LI-COR,) coupled to an IRGA (LI-8100A, LI-

COR) measured E_{floor} every 30 min on a permanently installed PVC collar. The automated chamber was deployed from winter 2013 to spring 2014 and rendered 222 days of measurements without errors (Figure S4). We found that E_{floor} measured with the clear chamber followed an exponential correlation with site E_p (Figure S4). Also, daily E_{floor} estimated from $\Delta\theta$ was significantly correlated with daily E_{floor} measured with the clear chamber ($p < .05$, Figure S4). For those dates with $P > 0$ mm per day and/or preceded by a day with $P \geq 2$ mm per day (276 days), E_{floor} was estimated from site E_p, from the exponential correlation of E_{floor} and E_p from the clear chamber measurements (Figure S4).

2.5 | Statistical analyses

We tested for significant differences ($p < .05$) between C_a levels over time on E_{tree}, E_{floor} and soil water storage by fitting general additive mixed models (GAMMs). For this purpose, we considered the ring as our experimental unit and assessed for random ring-to-ring variability within each C_a level (Wood, 2006). We used the *mgcv* package in R version 3.2.2 (R Development Core Team, 2014). In all fitted GAMMs, we used a cubic regression spline. For the smoothed term in the model, we used up to 5–20 degrees of freedom, which resulted in biologically realistic smoothed dynamics. Additionally, to quantify soil water dynamics under ambient and eC_a, irrespective of horizontal and vertical heterogeneity in soil texture, we estimated the numerical derivative of soil water storage (dS/dt) and its confidence interval (Duursma et al., 2016) as estimated from the GAMM fitted to dS/dt for ambient and eC_a, for the whole vertical profile (0–3 m) and for specific depths.

To assess the effect of eC_a on the relationships between climatic (D, T_{soil} and PAR) and other environmental drivers (θ_v and L) and transpiration components (E_i, E_{tree}, E_{floor}), we used either GAMMs or linear mixed models (LMM). We used a LMM to assess the effects of eC_a on the relationships of E_i with L; precipitation event duration and size; with ring and precipitation event as random factors. We used GAMMs to test for the effect of eC_a on the climatic forcing of E_{tree} and E_{floor}, with ring and date as random factors. For E_{tree}, we included D, u and PAR as predictors and L as a covariate (Duursma et al., 2014). To further asses the eC_a effect on the climatic forcing of E_{tree} we performed an additional GAMM with day-length normalized D (D_z, Tor-ngern et al., 2015). For E_{floor} (computed only from $\Delta\theta$ measured inside the rings), we included understorey D and PAR, T_{soil} and θ_v (Raz-Yaseef, Yakir, Schiller, & Cohen, 2012).

We estimated our ability to close the water balance by calculating P minus ($R + D_g + \Delta S + E_t$) from Equation 2. We computed the overall water balance for the study site, with site P, R, D_g and average ($n = 6$ rings) ΔS and E_t. We calculated the terms of the water balance for each season (summer, DJF; autumn, MAM; winter, JJA; and spring, SON). We considered that we had closed the water balance when the sum of the water balance components (Equation 2) was at least 75% of precipitation for that period, that is $|(P - R + D_g + \Delta S + E_t)/P| < 0.25$ (Schreiner-Mcgraw et al., 2016).

3 | RESULTS

3.1 | Meteorological parameters and precipitation

All the data and analyses presented in this manuscript are published here for the first time, except for the raw climatic data (temperature, precipitation and air relative humidity, Gimeno et al., 2016) and the leaf area index (L, Duursma et al., 2016). Prior to the start of the eC_a treatment, the EucFACE site experienced a very wet summer and early autumn (P_{cum} December 2011-April 2012: 647 mm, or 2/3rds of long-term annual average), followed by an average autumn and winter. During the eC_a ramp-up, the site experienced a wet and warm spring and summer, and a heat wave when we recorded the highest D on site for the study period (7.9 kPa, Figure 1). In late January 2013, the site received P_{cum} = 191 mm in 7 days (Figure 2) that led to temporary standing water on site for 48 h. The first year of full eC_a treatment (commencing on February 2013) was characterized by a warm and dry winter, followed by an unusually hot and dry early spring that boosted daily D and E_p close to typical midsummer values (Figure 1). This was followed by a rainy spring (P_{cum} = 218 mm in November 2013, Figure 2) that preceded a drier than usual summer (P_{cum} = 87 mm in February 2014) and finally an average autumn and winter in 2014 (Figure 1, Table 1).

3.2 | Surface runoff (R), drainage (D_g) and groundwater depth

Over the study period, P_{cum} exceeded maximum soil water storage capacity (108 mm) during one precipitation event (27 January 2013; Figure 2) with an excess of 39 mm over 24 hr. During this period E_p was 8 mm, so R was estimated as 31 mm (Table 1). Furthermore, the site experienced one event (15 November 2013) that should have exceeded soil infiltration capacity, but the soil was not saturated and standing water was absorbed before any R was generated.

From July 2013 to October 2014, mean groundwater depth was 12.8 m and ranged from 12.64 to 12.96 m. The variability in the groundwater depth did not show any daily or seasonal patterns (Figure S2). The isotopic signature of xylem water under dry and wet conditions did not match the signature of groundwater (Figure S3). These analyses, together with the absence of live roots below 1 m depth observed during the augering of 15 holes of 4.5 m depth each, suggests that the EucFACE deep-rooted vegetation (trees) did not access groundwater. Henceforth, we argue that observed changes in the groundwater depth were likely associated with regional groundwater—surface water interactions governed by the water level in the Hawkesbury River. Our approach to calculate D_g (Equation 3) should be valid for the temporal (2 years) and spatial (~1 ha of instrumented study area) scale of this study.

The contribution of D_g to the water balance varied from 20% (spring 2012) to 2% in summer 2013 (Table 1), although it should be noted that seasonal D_g and P could be temporally uncoupled. Coupling depends on the P dynamics and the level of antecedent saturation in the soil column. At our site, D_g might be lagged with respect

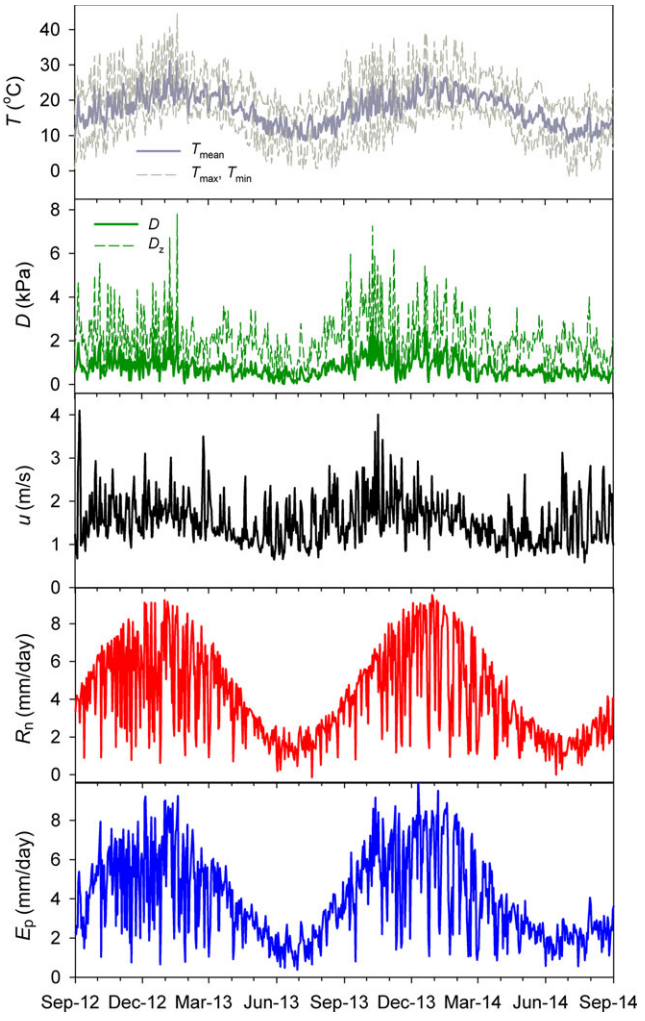

FIGURE 1 Meteorological variables during the study period from top to bottom: maximum (T_{max}) and minimum (T_{min}) daily temperatures (dashed grey lines), mean daily temperature (T_{mean}); mean daily water pressure deficit (D, continuous green line) and day-length normalized D ($D_z = D\ n_d/24$, where n_d is the number of daylight hours dashed green line); mean daily wind speed (u); total net radiation (R_n) and total Penman potential evapotranspiration (E_p)

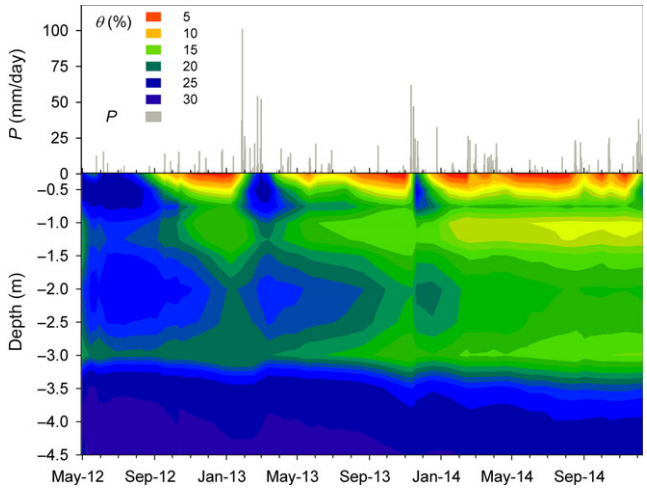

FIGURE 2 Daily precipitation (P, grey bars) and temporal evolution of the vertical profile of soil volumetric water content (θ) inferred from mean (n = 6 rings) periodical measurements

to seasonal P when the upper soil column (0–3 m, sand and sandy clay loam) was saturated with water, but not the deep soil (below 3 m, clay). This would have led to an initial increase in deep soil water storage that would have later drained below the root zone. This was the case in autumn 2013 when D_g according to our calculation was negative (i.e. apparent reduction in the amount of water below the root zone). With the exception of this latter season, our approach showed that over the study period, there was an excess of water draining beyond the root zone.

3.3 | Effect of elevated CO_2 on soil water storage (S)

Initial measurements of S (June 2012) were the maximum over the study period. S_{max} varied among rings due to differences in soil texture (ring 6 with the highest clay content had the highest S_{max}: 828 mm) and microtopography (S_{max} in ring 5 with the lowest elevation was 758 mm, while in ring 1: 657 mm). We found that S decreased continuously in all rings during 2012, until early 2013, when large precipitation events increased S close to S_{max} (Figures 2 and 3a). In 2013, S also decreased until another series of precipitation events in November, when S increased, but did not reach S_{max} (Figure 3a). During the first half of 2014, S decreased until a series of precipitation events in the middle of the year (August) interrupted this trend (Figure 3a), yet S did not reach S_{max}. The complete overlapping of the 95% CI of the fitted GAMM to S over time between C_a levels indicated that there were no significant differences in S between C_a levels (Figure 3a). Similarly, we found that S integrated over 0.25 or 0.5 m depth intervals did not differ between C_a (Figure S5).

We found that S decreased significantly for most of the study period, ($dS/dt < 0$, $p < .05$), particularly during the autumn-winter (Figure 3b). During wet periods, S increased, but dS/dt was significantly positive only in summer 2013 and spring 2014. The 95% CI of the fitted GAMM for ambient and eC_a overlapped over the entire period, indicating that there were no significant differences in dS/dt (Figure 3b). We found similar results for dS/dt calculated for specific depths up to 2 m (Figure S6). Below 2 m depth, in 2012 (pretreatment and ramp-up), dS/dt in eC_a was positive or zero when our measurements commenced and then it declined progressively to stable negative values, nonsignificantly different from those in ambient C_a. This result was strongly driven by the contrasting trends observed in two of the study rings that happened to be randomly assigned to different C_a levels and it is not likely to have been generated by the eC_a treatment per se. Instead, this resulted from the preceding heavy rainfall that most likely led to lateral water redistribution towards ring 5, which has the lowest elevation and which happened to be randomly assigned to the eC_a treatment. Additionally, this could have also resulted from a greater rate of soil water decline observed in

TABLE 1 Total seasonal potential evapotranspiration (E_p), precipitation (P), surface runoff (R), drainage (D_g) change in soil water storage (ΔS) and total evapotranspiration (E_t)

Season	CO_2	E_p	P	R	ΔS	E_t	E_i	E_{tree}	E_{floor}
Spring-2012	a	429	92	0	−106 ± 10	97 ± 5	10 ± 2	64 ± 3	23 ± 1
	e				−109 ± 23	108 ± 20	17 ± 9	68 ± 11	23 ± 1
Summer-2013	a	486	377	31	133 ± 17	190 ± 22	47 ± 9	109 ± 15	35 ± 2
	e				119 ± 26	206 ± 32	50 ± 10	122 ± 21	33 ± 2
Autum-2013	a	296	155	0	−113 ± 13	153 ± 9	20 ± 1	99 ± 12	34 ± 4
	e				−89 ± 26	151 ± 21	24 ± 7	100 ± 18	28 ± 3
Winter-2013	a	197	84	0	−45 ± 17	84 ± 9	3 ± 1	61 ± 8	19 ± 1
	e				−48 ± 18	81 ± 10	5 ± 2	57 ± 11	19 ± 1
Spring-2013	a	488	250	0	114 ± 40	120 ± 13	21 ± 8	75 ± 6	24 ± 1
	e				110 ± 40	126 ± 16	32 ± 8	69 ± 12	24 ± 1
Summer-2014	a	536	151	0	−149 ± 30	159 ± 10	16 ± 4	106 ± 8	36 ± 1
	e				−139 ± 23	172 ± 23	23 ± 6	111 ± 21	38 ± 4
Autum-2014	a	275	170	0	−26 ± 12	132 ± 3	30 ± 7	76 ± 9	27 ± 2
	e				−34 ± 4	142 ± 22	28 ± 5	89 ± 17	15 ± 1
Winter-2014	a	195	150	0	25 ± 3	80 ± 6	18 ± 1	50 ± 6	13 ± 0.2
	e				14 ± 4	87 ± 11	20 ± 6	54 ± 12	13 ± 0.5

E_t is the sum of canopy interception (E_i), canopy transpiration (E_{tree}) and soil evaporation and understorey transpiration (E_{floor}). E_p, P, R and D_g were measured or calculated at the site level. Depicted values of ΔS, E_t, E_i, E_{tree} and E_{floor} are the mean (±SE) of the three rings for each atmospheric CO_2 level (ambient, a, and elevated, e). There were no significant differences ($p > .01$) between CO_2 levels for any of the hydrological components. All values in mm per season.

one of the ambient C_a rings (ring 6), which was not mimicked by the other two ambient rings (2 and 3), but yet affected the overall mean of the ambient C_a treatment. We suggest that vertical heterogeneity in the soil texture structure was responsible for differences among ambient C_a rings.

3.4 | Stem flow (S_f), throughflow (T_f) and interception (E_i) under elevated CO_2

We found that S_f, measured adjacent to the EucFACE rings, was significantly correlated ($p < .001$) to tree basal area, and the quantity and duration of P events (Table S1). The estimated contribution of S_f within each ring was <2% of precipitation.

E_i did not differ between C_a levels (Table 2). The best model for E_i included L, quantity and duration of the P event, but it did not include C_a, or its interactions (Table 2). Since L did not respond to eC_a, indirect eC_a effects on E_i were discarded. Across the seasons, the contribution of E_i to E_t was not negligible (Figure 4) and ranged from 5% (in winter 2013) to 24% (summer 2013). The main driver of E_i was P_{cum} (Table 2) so differences in the relative contribution of E_i to E_t between years and within season were due to differences in P (Figure 4 and Table S2).

3.5 | Canopy transpiration (E_{tree}) and understorey evapotranspiration (E_{floor}) under elevated CO_2

A leaf flushing event occurred shortly after the start of the implementation of the full eC_a treatment, thus the potential direct effect of eC_a on leaf-level transpiration would have been realized since the beginning of the experimental treatment. Over the study period, neither E_{tree}, nor E_{floor} differed between C_a levels, as evidenced by the consistent overlap of the 95% GAMMs confidence intervals (Figures 5 and 6, Figures S7 and S8). E_{tree} constituted the largest proportion of seasonal E_t, followed by E_{floor}, in all seasons (Figure 4). The mean contributions of E_{tree} and E_{floor} to E_t were 63% and 20%, respectively, and ranged from 72% (winter 2013) to 58% (summer 2013) for E_{tree} and from 23% (spring 2013) to 15% (winter 2014) for E_{floor}. Daily E_{tree} showed the typical three-phase response to D_z variation, initially rising with increasing D_z until it reached a plateau and then decreasing, with no significant differences between C_a levels (Figure 6). The GAMM also showed that E_{tree} was strongly driven by total daily PAR, again with no significant differences between C_a levels (Figure S7). E_{floor} was strongly controlled by θ_v followed by T_{soil} and understorey D with no significant differences between C_a levels (Figure S8).

3.6 | The overall water balance

We quantified the water balance components for our site and according to our criteria, $|(P - R - D_g - \Delta S - E_t)/P| < 0.25$, we achieved good closure in summer and spring 2013 and in winter 2014. Also, we were able to account for 44% of P in winter 2013 (Table 3). We were unable to close the water balance in spring 2012, autumn 2013 and summer 2014; three seasons preceded by large precipitation events (Figure 2), when soil water storage increased by more than 100 mm (Table 1).

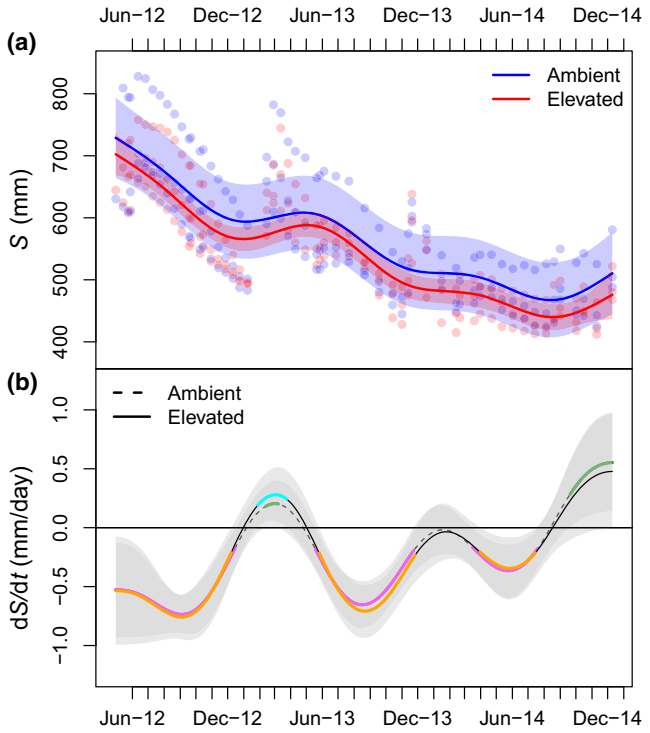

FIGURE 3 (a) Soil water storage (S) over a soil column of 3 m depth, each point is the mean of two locations within each ring, lines and polygons represent the fitted generalized additive models with their 95% confidence intervals (CI) for each CO_2 treatment level. (b) Mean estimated daily changes in S (dS/dt, lines) and 95% CIs (polygons). Rates of change not significantly different from 0 are indicated with dashed (ambient) or continuous (elevated) black lines. Significantly negative changes are indicated with pink (ambient) and orange (elevated) lines and positive changes with cyan (elevated) and green (ambient) lines

TABLE 2 Results (estimated coefficients ± SE, t and p-value) of the best linear mixed model fit to canopy interception (E_i, log-transformed)

Fixed	Estimate	t	p
Log (P_{cumm})	0.322 ± 0.02	15.2	<.001
Duration	0.03 ± 0.006	5.5	<.001
L	−0.18 ± 0.09	−2.1	.038

Selected fixed factors were: event precipitation (P_{cum} in mm, log-transformed), event duration (in h) and leaf area index (L, in m^2 per m^2). The CO_2 treatment did not significantly affect E_i or the any of the effect sizes.

4 | DISCUSSION

Our study constitutes the most comprehensive quantification of the hydrological balance of a tree-dominated FACE experiment (Leuzinger & Körner, 2010; Schäfer et al., 2002). Previous forest FACE studies found reduced tree water-use (Warren et al., 2011) but neglected the eC_a effect on understorey evapotranspiration (except from Schäfer et al., 2002) or on the partitioning to ΔS, D_g and R. Furthermore, none of these were conducted in water-limited sites and while some climatic land-surface models predict an increase in ΔS and eventually in R and D_g (Betts et al., 2007; Gedney et al., 2006); this prediction does not appear to hold for water-limited regions (Ukkola et al., 2016). Furthermore, all these predictions are based on retrospective analyses and thus are limited to present-day C_a and cannot account for projected C_a increases for most of the 21st century. For water-limited regions, process-based theoretical models predict that increased L offsets reduced leaf-level transpiration under eC_a (Donohue et al., 2017; Macinnis-Ng et al., 2011). Here, for our water-limited woodland, we had hypothesized that reduced E_{tree} under eC_a, would not be offset by increased L (Duursma et al., 2016) and since the site is water-limited, any excess water resulting from reduced E_{tree} would be quickly lost via E_{floor}, meaning no net increase in ΔS. We found no changes in E_{tree}, E_{floor} or ΔS, thus eC_a did not reduce stand water-use in this mature water-limited woodland.

4.1 | Canopy transpiration under ambient and elevated CO_2

Contrary to our expectations, we did not find a reduction in E_{tree} under eC_a, neither in daily mean nor maximum v_s. Some previous forest FACE studies had found nonsignificant reductions in E_{tree} under eC_a (Bobich et al., 2010; Ward et al., 2013); but in these studies, reductions in leaf-level transpiration were offset by increased L, which we did not observe (Duursma et al., 2016). In our case, g_s of the canopy-dominant tree (*E. tereticornis*) temporary decreased by 20%, but this reduction was transient and became nonsignificant when water availability became most limiting and D peaked (Gimeno et al., 2016). Furthermore, any given decrease in g_s is usually translated into a weaker transpiration response because there are additional sources of variability affecting the upscaling from leaf- to canopy-level processes such as micrometeorology, canopy patchiness and/or vertical variations in leaf anatomy, even in well-coupled canopies, such as ours (Jarvis & Mcnaughton, 1986). Hence, it is not surprising that the partial reduction observed in g_s from discrete campaigns restricted to the upper part of dominant trees did not scale to the canopy level. Additionally, our observations from this native woodland are inherently affected by the natural variability. For example, the mean coefficient of variation for mean daily v_s within rings (i.e. among trees) was 38%, whereas within C_a levels (i.e. among rings) it was 24%, despite selection of the most representative and comparable trees that contributed up to 50% of the total basal area within each ring. Given that maximum measured reduction in g_s was 20% (Gimeno et al., 2016); we cannot discard that potential transient reductions in canopy transpiration could have been obscured by the natural variability among trees for this 2 year study (Paschalis, Katul, Fatichi, Palmroth, & Way, 2017).

Besides the expected direct effect of eC_a on E_{tree}, we also expected indirect effects, beyond changes in L that did not occur (Duursma et al., 2016). Elevated C_a could have also indirectly affected E_{tree} by modifying climatic forcing of transpiration; for

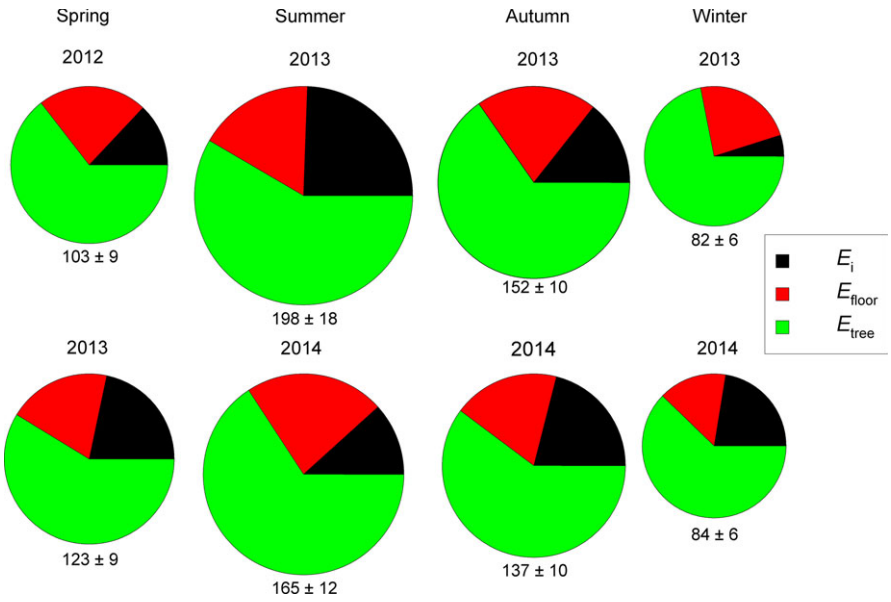

FIGURE 4 Partitioning of total evapotranspiration among: canopy interception (E_i), canopy transpiration (E_{tree}) and understorey transpiration together with floor evaporation (E_{floor}). The size of each pie-chart is proportional to the corresponding seasonal evapotranspiration (in mm per season) indicated (site mean ± *SE*, $n = 6$ rings)

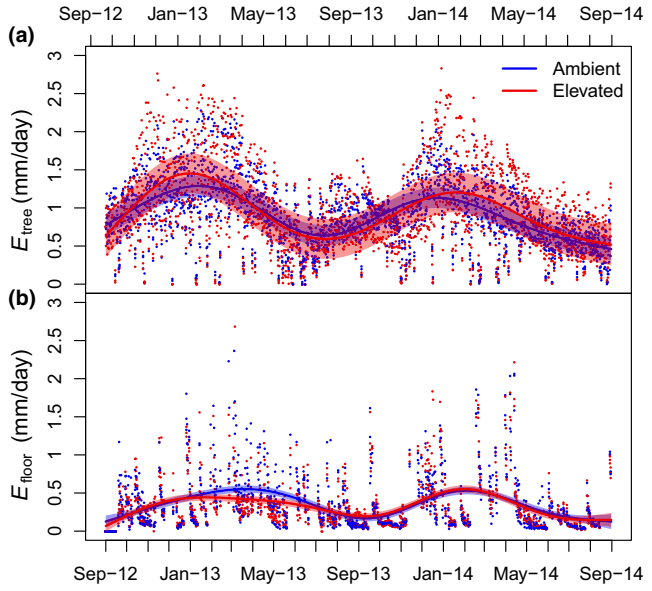

FIGURE 5 (a) Estimated daily canopy tree transpiration (E_{tree}) and (b) understorey evapotranspiration (E_{floor}) for each ring under different C_a concentrations levels: ambient (blue) and elevated (red). Lines and polygons represent the fit of the GAMMs for each C_a level with their 95% confidence intervals. E_{tree} was estimated from mean (n = 3–4 trees per ring) sapflow velocities and E_{floor} was estimated from mean (n = 2 locations per ring) changes in shallow (5 cm) soil volumetric water content

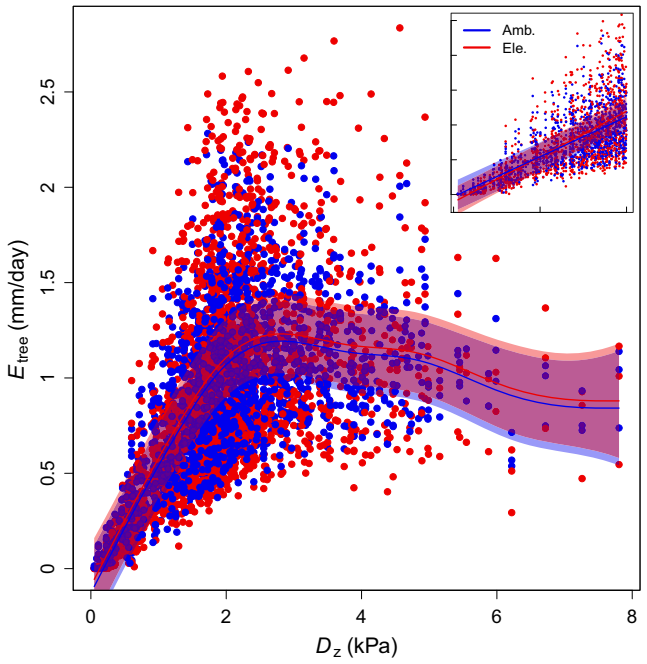

FIGURE 6 Estimated daily canopy tree transpiration (E_{tree}) under different CO_2 concentrations: ambient (blue) and elevated (red) plotted against day-length normalized mean daily vapour pressure deficit (D_z). Lines and polygons represent the estimated fit of the GAMMs for each CO_2 level with their 95% confidence intervals (CI). E_{tree} was estimated from mean (n =3–4 trees per ring) sapflow velocities. Figure inset represent the fits and CIs of a linear mixed model restricted to $D_z < 2$ kPa, where daily E_{tree} increased linearly with D_z ($t = 20.6$, $p < .01$) and depicted lines have slopes (±*SE*) of 0.57 ± 0.03 and 0.67 ± 0.01 mm day^{-1} kPa^{-1}, for ambient and elevated CO_2 levels respectively

example, the slope of the relationship between D and transpiration can decrease under eC_a (Duursma et al., 2014; Wullschleger & Norby, 2001). In our study, there were no significant differences between C_a levels in the response of E_{tree} to D, including a much lar-

TABLE 3 Seasonal values of the ratio of precipitation (P) to potential evapotranspiration (E_p), P, surface runoff (R), drainage (D_g) change in soil water storage (ΔS) and total evapotranspiration (E_t)

Year	2012	2013				2014		
Season	Spring	Summer	Autumn	Winter	Spring	Summer	Autumn	Winter
P/E_p	0.21	0.78	0.53	0.42	0.51	0.28	0.62	0.77
P	92	377	155	84	250	151	170	150
R	0	31	0	0	0	0	0	0
D_g	19	6	−4	11	20	18	4	11
ΔS	−107 (11)	126 (14)	−101 (14)	−47 (11)	112 (25)	−144 (17)	−30 (6)	19 (3)
E_t	103 (9)	198 (18)	152 (10)	82 (6)	123 (9)	165 (12)	137 (10)	84 (6)
Error	78	16	108	37	−5	111	58	36
|Error/P|	0.84	0.04	0.69	0.44	0.02	0.74	0.34	0.24

For terms measured at the ring level (ΔS and E_t), depicted values are the mean (SE) of the six rings. The error denotes the disequilibrium from the closure of the water balanced calculated as: $P - R - D_g - \Delta S - E_t = 0$. All values, except for P/E_p and |Error/P| (both unitless), are in mm per season

ger D (up to 7.9 kPa) than experienced previously at another forested FACE experiment (Tor-ngern et al., 2015). This result is consistent with the lack of a significant effect of eC_a on the combined sensitivity of stomata to C_a and D in eucalypts (Gimeno et al., 2016; Kelly, Duursma, Atwell, Tissue, & Medlyn, 2016). Taken together, these results suggest that eC_a is unlikely to alleviate increasing atmospheric drought stress in a climate change scenario with warmer temperatures and higher D (Nelson et al., 2004), at least in this mature eucalypt woodland.

4.2 | Understorey evapotranspiration and canopy interception under elevated CO_2

We had hypothesized that excess water resulting from reduced E_{tree} under eC_a would be lost via enhanced E_{floor}, but here, E_{tree} did not decrease under eC_a and there was no increase in E_{floor}. Consistently, soil water storage (S) did not differ between ambient and eC_a plots at any depth and neither did ΔS over the study period, which vertically extends similar results for the upper soil (0–30 cm) on the same site (Drake et al., 2016; Pathare et al., 2017). Previous studies had reported that soil moisture was not conserved in eC_a in water-limited regions (Nowak et al., 2004) and without increased water availability; it is not surprising that there was no change in E_{floor}. We did not find an indirect effect on E_{floor} either, as the response of E_{floor} to T_{soil} and θ_v was unaffected by eC_a. With our approach, we cannot separate the contributions of understorey transpiration and soil evaporation to E_{floor}, which in this type of woodland are both likely to constitute an important fraction of ecosystem water-use (Ferretti et al., 2003; Nolan et al., 2014). In our study, the evaporative component could not have been affected by eC_a because soil water did not increase (Drake et al., 2016) and the amount of incident radiation in the understorey did not decrease, as L was unaffected (Duursma et al., 2016). In contrast, we could have still expected that transpiration by the understorey responded to eC_a, in addition to indirect environmental effects (via changes in soil moisture or incident radiation). Nevertheless, 3 years of measurements on the dominant understorey grasses on-site revealed that under eC_a neither g_s decreased, nor did herbaceous biomass increase (Collins et al., 2018; Pathare et al., 2017).

We quantified the contribution of E_i to E_t and whether this component changed under eC_a. In agreement with previous studies (Crockford & Richardson, 2000; Gash, 1979; Soubie, Heinesch, Granier, Aubinet, & Vincke, 2016), quantity and duration of the P events were the main drivers of E_i, T_f and S_f. More abundant and longer events resulted into larger E_i, but contrary to expectations, we found a negative effect of L on E_i. The prediction that E_i increases with L is based on observations from densely packed canopies with horizontally angled leaves (Kergoat, 1998). However, in most *Eucalypt* woodlands, including ours, leaves are angled vertically or near-vertically; hence, P falling on the vegetation mostly contributes to T_f instead of E_i (Crockford & Richardson, 2000). Nevertheless, given that neither L (Duursma et al., 2016) nor tree radial growth rate increased under eC_a (Ellsworth et al., 2017), we are unlikely to observe any change in the partitioning of P into T_f, S_f and E_i under eC_a, in mature *Eucalypt* woodlands. Even under a scenario where L and/or growth responded to eC_a, we would still predict that E_i would not change because the contribution of S_f is negligible (and thus so would be potential increases in S_f due to radial growth increments) and greater L would not increase E_i with these leaf angles. This later result is relevant for improving our ability to estimate ecosystem water-use and to predict vegetation–atmospheric coupling under future atmospheric conditions. Currently, most process-based models assume that E_i increases with eC_a (De Kauwe et al., 2013; Zhang et al., 2016), but our results suggest otherwise for this type of woodland, over the study period.

4.3 | Lack of effective water-savings under elevated CO_2

Over the study period, potential evapotranspiration (E_p) exceeded precipitation (P) in all seasons and total E_t was always less than E_p, which indicates that our site was water-limited during the study period, at this time step. We found that despite being water-limited, seasonal E_t was often less than P, which allowed some P to be partitioned to ΔS, R

and D_g. Here, we followed a conservative approach to calculate D_g from deep soil water dynamics assuming an effective rooting depth of 3 m. With this approach, we are likely overestimating the decrease in ΔS and thus we are underestimating the amount partitioned to D_g. For those seasons where we calculated a decrease in ΔS, our estimate of E_t was not similar to ΔS plus P, minus R and D_g. Our estimates of E_{tree} and E_{floor} are comparable to observations from similar (Nolan et al., 2014) and nearby forests (Bourne, Haigh, & Ellsworth, 2015) and the proportion of seasonal E_i is within the range of other studies (Kergoat, 1998; Soubie et al., 2016). Hence, it is not reasonable to believe that we largely underestimated E_t (by nearly 100%). A more plausible explanation is that we overestimated the effective rooting depth (Macinnis-Ng et al., 2010), but without a detailed survey of root distribution we are unable to provide a more realistic ΔS. This latter explanation would agree with the estimates from a recent modelling study (Yang, Donohue, & McVicar, 2016), which estimated an effective rooting depth of 1.2 m in the region. Here, we opted for a more conservative approach and established an effective rooting depth based our own observations and characterization of the soil texture profile. Nevertheless, despite the uncertainty regarding effective rooting depth, we found that eC_a had no effect on the temporal dynamics of S or ΔS at any depth during the entire study period, further supporting our argument that eC_a did not increased soil water storage at any depth, in this woodland.

In addition to our estimate of rooting depth, there may be other sources of uncertainty, such as our coarse approach to estimate R from measurements of P and soil properties. We established that R would only occur at times when the soil was fully saturated and precipitation exceeded the infiltration capacity, yet since EucFACE occurs on an alluvial floodplain, soil saturation may not occur homogeneously across the site. Indeed, some unquantified R might have been generated in areas where the soil saturated faster than the overall site mean due to spatial heterogeneity in soil texture. Furthermore, we did not account for the contribution of possible deep lateral flow that can occur in multilayered strongly contrasting textured soils (Cox & Pitman, 2002), such as at our site. These uncertainties could explain our inability to fully close the overall water balance for our study site for those seasons preceded by very rainy season, when we would have been more likely to underestimate D_g, R and lateral flow.

We examined the impact of eC_a on the hydrological balance of a native, mature woodland at the stand level for 30 months and during periods of water-limitation. Elevated C_a did not alter ΔS, E_{tree}, E_{floor}, E_i or E_t during this time Furthermore, eC_a did not indirectly affect E_t through changes in growth, phenology or L. In addition, we did not find significant effects of eC_a on the climatic forcing of transpiration, such that under a future climate change scenario (i.e. altered precipitation patterns and warmer global surface temperatures), more severe water-stress due to an increase in evaporative demand would not be alleviated under eC_a in this type of woodland. Based on this study, in water-limited catchments dominated by mature woodlands we should not expect changes in the amounts of precipitation partitioned to R and D_g in response to future increases in C_a.

ACKNOWLEDGEMENTS

Many thanks to Remko Duursma for his assistance with field data collection (leaf area index) and data analyses. Thanks also to Burhan Amiji, Craig Barton, Catherine Beattie, Vinod Kumar, Craig McNamara, Lindsay Nicks and Steven Wohl for their valuable contributions to our field work. We greatly acknowledge Margaret Barbour and Kevin Simonin for assistance in soil sample preparation for isotopic analysis at the University of Sydney; to David G. Williams and Craig Cook for sample processing and isotopic analyses at the University of Wyoming. Thanks to Belinda Medlyn and the ECOFUN team for constructive comments during manuscript preparation. EucFACE is supported by the Australian Commonwealth Government in collaboration with the Western Sydney University (WSU). EucFACE was built as an initiative of the Australian Government as part of the Nation-building Economic Stimulus Package. TEG was funded by a research collaborative agreement between CSIRO and WSU within the CSIRO Flagship programme "Water for a Healthy Country" during this research, and funded by the IdEx programme of the Université de Bordeaux and a Marie Skłodowska-Curie Intra-European fellowship (Grant Agreement No. 653223) during manuscript preparation. Thanks to the three anonymous reviewers and the editor for comments that improved our original submission. All data used in the manuscript are stored in the institutional archive of the Western Sydney University and publicly available (http://doi.org/10.4225/35/5ab9bd1e2f4fb).

ORCID

Teresa E. Gimeno http://orcid.org/0000-0002-1707-9291
Tim R. McVicar http://orcid.org/0000-0002-0877-8285
David T. Tissue http://orcid.org/0000-0002-8497-2047
David S. Ellsworth http://orcid.org/0000-0002-9699-2272

REFERENCES

Aston, A. R. (1984). The effect of doubling atmospheric CO_2 on streamflow - A simulation. *Journal of Hydrology*, *67*, 273–280. https://doi.org/10.1016/0022-1694(84)90246-4

Betts, R. A., Boucher, O., Collins, M., Cox, P. M., Falloon, P. D., Gedney, N., & Webb, M. J. (2007). Projected increase in continental runoff due to plant responses to increasing carbon dioxide. *Nature*, *448*, 1037–U1035. https://doi.org/10.1038/nature06045

Bobich, E. G., Barron-Gafford, G. A., Rascher, K. G., & Murthy, R. (2010). Effects of drought and changes in vapour pressure deficit on water relations of *Populus deltoides* growing in ambient and elevated CO_2. *Tree Physiology*, *30*, 866–875. https://doi.org/10.1093/treephys/tpq036

Bourne, A. E., Haigh, A. M., & Ellsworth, D. S. (2015). Stomatal sensitivity to vapour pressure deficit relates to climate of origin in *Eucalyptus* species. *Tree Physiology*, *35*, 266–278. https://doi.org/10.1093/treephys/tpv014

Campbell, G. S., & Norman, J. M. (1998). *An introduction to environmental biophysics*. New York, NY: Springer. https://doi.org/10.1007/978-1-4612-1626-1

Cech, P. G., Pepin, S., & Körner, C. (2003). Elevated CO_2 reduces sap flux in mature deciduous forest trees. *Oecologia*, *137*, 258–268. https://doi.org/10.1007/s00442-003-1348-7

Cheng, L., Zhang, L., Wang, Y. P., Canadell, J. G., Chiew, F. H., Beringer, J., & Zhang, Y. (2017). Recent increases in terrestrial carbon uptake at little cost to the water cycle. *Nature Communications*, *8*, 110. https://doi.org/10.1038/s41467-017-00114-5

Cheng, L., Zhang, L., Wang, Y. P., Yu, Q., Eamus, D., & O'Grady, A. (2014). Impacts of elevated CO_2, climate change and their interactions on water budgets in four different catchments in Australia. *Journal of Hydrology*, *519*, 1350–1361. https://doi.org/10.1016/j.jhydrol.2014.09.020

Collins, L., Bradstock, R. A., Resco De Dios, V., Duursma, R. A., Velasco, S., & Boer, M. M. (2018). Understorey productivity in temperate grassy woodland responds to soil water availability but not to elevated [CO_2]. *Global Change Biology*. https://doi.org/10.1111/gcb.14038

Cox, J. W., & Pitman, A. J.(2002). The water balance of pastures in a South Australian catchment with sloping texture-contrast soils. In T. R. McVicar, L. Rui, J. Walker, R. W. Fitzpatrick & L. Changming (Eds.), *Regional water and soil assessment for managing sustainable agriculture in China and Australia* (pp. 82–94). Canberra, ACT: Australian Centre for International Agricultural Research.

Crockford, R. H., & Richardson, D. P. (2000). Partitioning of rainfall into throughfall, stemflow and interception: Effect of forest type, ground cover and climate. *Hydrological Processes*, *14*, 2903–2920. https://doi.org/10.1002/(ISSN)1099-1085

De Kauwe, M. G., Medlyn, B. E., Zaehle, S., Walker, A. P., Dietze, M. C., Hickler, T., & Smith, B. (2013). Forest water use and water use efficiency at elevated CO_2: A model-data intercomparison at two contrasting temperate forest FACE sites. *Global Change Biology*, *19*, 1759–1779. https://doi.org/10.1111/gcb.12164

Donohue, R. J., McVicar, T. R., & Roderick, M. L. (2009). Climate-related trends in Australian vegetation cover as inferred from satellite observations, 1981-2006. *Global Change Biology*, *15*, 1025–1039. https://doi.org/10.1111/j.1365-2486.2008.01746.x

Donohue, R. J., McVicar, T. R., & Roderick, M. L. (2010). Assessing the ability of potential evaporation formulations to capture the dynamics in evaporative demand within a changing climate. *Journal of Hydrology*, *386*, 186–197. https://doi.org/10.1016/j.jhydrol.2010.03.020

Donohue, R. J., Roderick, M. L., McVicar, T. R., & Yang, Y. T. (2017). A simple hypothesis of how leaf and canopy-level transpiration and assimilation respond to elevated CO_2 reveals distinct response patterns between disturbed and undisturbed vegetation. *Journal of Geophysical Research-Biogeosciences*, *122*, 168–184. https://doi.org/10.1002/2016JG003505

Drake, J. E., Macdonald, C. A., Tjoelker, M. G., Crous, K. Y., Gimeno, T. E., Singh, B. K., & Ellsworth, D. S. (2016). Short-term carbon cycling responses of a mature eucalypt woodland to gradual stepwise enrichment of atmospheric CO_2 concentration. *Global Change Biology*, *22*, 380–390. https://doi.org/10.1111/gcb.13109

Duursma, R. A., Barton, C. V., Eamus, D., Medlyn, B. E., Ellsworth, D. S., Forster, M. A., & McMurtrie, R. E. (2011). Rooting depth explains CO_2 x drought interaction in *Eucalyptus saligna*. *Tree Physiology*, *31*, 922–931. https://doi.org/10.1093/treephys/tpr030

Duursma, R. A., Barton, C. V., Lin, Y. S., Medlyn, B. E., Eamus, D., Tissue, D. T., & McMurtrie, R. E. (2014). The peaked response of transpiration rate to vapour pressure deficit in field conditions can be explained by the temperature optimum of photosynthesis. *Agricultural and Forest Meteorology*, *189*, 2–10. https://doi.org/10.1016/j.agrformet.2013.12.007

Duursma, R. A., Gimeno, T. E., Boer, M. M., Crous, K. Y., Tjoelker, M. G., & Ellsworth, D. S. (2016). Canopy leaf area of a mature evergreen *Eucalyptus* woodland does not respond to elevated atmospheric CO_2 but tracks water availability. *Global Change Biology*, *22*, 1666–1676. https://doi.org/10.1111/gcb.13151

Ellsworth, D. S. (1999). CO_2 enrichment in a maturing pine forest: Are CO_2 exchange and water status in the canopy affected? *Plant Cell and Environment*, *22*, 461–472. https://doi.org/10.1046/j.1365-3040.1999.00433.x

\Ellsworth, D. S., Anderson, I. C., Crous, K. Y., Cooke, J., Drake, J. E., Gherlenda, A. N., & Tjoelker, M. G. (2017). Elevated CO_2 does not increase eucalypt forest productivity on a low-phosphorus soil. *Nature Climate Change*, *7*, 279–282. https://doi.org/10.1038/nclimate3235

Ellsworth, D. S., Thomas, R., Crous, K. Y., Palmroth, S., Ward, E., Maier, C., & Oren, R. (2012). Elevated CO_2 affects photosynthetic responses in canopy pine and subcanopy deciduous trees over 10 years: A synthesis from Duke FACE. *Global Change Biology*, *18*, 223–242. https://doi.org/10.1111/j.1365-2486.2011.02505.x

Fatichi, S., Leuzinger, S., Paschalis, A., Langley, J. A., Barraclough, A. D., & Hovenden, M. J. (2016). Partitioning direct and indirect effects reveals the response of water-limited ecosystems to elevated CO_2. *Proceedings of the National Academy of Sciences of the United States of America*, *113*, 12757–12762. https://doi.org/10.1073/pnas.1605036113

Ferretti, D. F., Pendall, E., Morgan, J. A., Nelson, J. A., Lecain, D., & Mosier, A. R. (2003). Partitioning evapotranspiration fluxes from a Colorado grassland using stable isotopes: Seasonal variations and ecosystem implications of elevated atmospheric CO_2. *Plant and Soil*, *254*, 291–303. https://doi.org/10.1023/A:1025511618571

Field, C. B., Jackson, R. B., & Mooney, H. A. (1995). Stomatal responses to increased CO_2 - Implications from the plant to the global scale. *Plant Cell and Environment*, *18*, 1214–1225. https://doi.org/10.1111/j.1365-3040.1995.tb00630.x

Fisher, J. B., Melton, F., Middleton, E., Hain, C., Anderson, M., Allen, R., & Kilic, A. (2017). The future of evapotranspiration: Global requirements for ecosystem functioning, carbon and climate feedbacks, agricultural management, and water resources. *Water Resources Research*, *53*, 2618–2626. https://doi.org/10.1002/2016WR020175

Gash, J. H. C. (1979). An analytical model of rainfall interception by forests. *Quarterly Journal of the Royal Meteorological Society*, *105*, 43–55. https://doi.org/10.1002/(ISSN)1477-870X

Gedney, N., Cox, P. M., Betts, R. A., Boucher, O., Huntingford, C., & Stott, P. A. (2006). Detection of a direct carbon dioxide effect in continental river runoff records. *Nature*, *439*, 835–838. https://doi.org/10.1038/nature04504

Gimeno, T. E., Crous, K. Y., Cooke, J., O'Grady, A. P., Ósvaldsson, A., Medlyn, B. E., & Ellsworth, D. S. (2016). Conserved stomatal behaviour under elevated CO_2 and varying water availability in a mature woodland. *Functional Ecology*, *30*, 700–709. https://doi.org/10.1111/1365-2435.12532

Godbold, D., Tullus, A., Kupper, P., Sõber, J., Ostonen, I., Godbold, J. A., … Smith, A. R. (2014). Elevated atmospheric CO_2 and humidity delay leaf fall in Betula pendula, but not in *Alnus glutinosa* or *Populus tremula x tremuloides*. *Annals of Forest Science*, *71*, 831–842. https://doi.org/10.1007/s13595-014-0382-4

Gunderson, C. A., Sholtis, J. D., Wullschleger, S. D., Tissue, D. T., Hanson, P. J., & Norby, R. J. (2002). Environmental and stomatal control of photosynthetic enhancement in the canopy of a sweetgum (*Liquidambar styraciflua* L.) plantation during 3 years of CO_2 enrichment. *Plant Cell and Environment*, *25*, 379–393. https://doi.org/10.1046/j.0016-8025.2001.00816.x

Huntington, T. G. (2008). CO_2-induced suppression of transpiration cannot explain increasing runoff. *Hydrological Processes*, *22*, 311–314. https://doi.org/10.1002/(ISSN)1099-1085

Jackson, R. B., Sala, O. E., Paruelo, J. M., & Mooney, H. A. (1998). Ecosystem water fluxes for two grasslands in elevated CO_2: A modeling analysis. *Oecologia*, *113*, 537–546. https://doi.org/10.1007/s004420050407

Jarvis, P. G., & Mcnaughton, K. G. (1986). Stomatal control of transpiration – Scaling up from leaf to region. *Advances in Ecological Research*, *15*, 1–49.

Keel, S. G., Pepin, S., Leuzinger, S., & Körner, C. (2007). Stomatal conductance in mature deciduous forest trees exposed to elevated CO_2.

Trees-Structure and Function, *21*, 151–159. https://doi.org/10.1007/s00468-006-0106-y

Keenan, T. F., Hollinger, D. Y., Bohrer, G., Dragoni, D., Munger, J. W., Schmid, H. P., & Richardson, A. D. (2013). Increase in forest water-use efficiency as atmospheric carbon dioxide concentrations rise. *Nature*, *499*, 324–327. https://doi.org/10.1038/nature12291

Kelly, J. W. G., Duursma, R. A., Atwell, B. J., Tissue, D. T., & Medlyn, B. E. (2016). Drought × CO_2 interactions in trees: A test of the low-intercellular CO_2 concentration (C_i) mechanism. *New Phytologist*, *209*, 1600–1612. https://doi.org/10.1111/nph.13715

Kergoat, L. (1998). A model for hydrological equilibrium of leaf area index on a global scale. *Journal of Hydrology*, *212*, 268–286. https://doi.org/10.1016/S0022-1694(98)00211-X

Leuzinger, S., & Körner, C. (2007). Water savings in mature deciduous forest trees under elevated CO_2. *Global Change Biology*, *13*, 2498–2508. https://doi.org/10.1111/j.1365-2486.2007.01467.x

Leuzinger, S., & Körner, C. (2010). Rainfall distribution is the main driver of runoff under future CO_2-concentration in a temperate deciduous forest. *Global Change Biology*, *16*, 246–254. https://doi.org/10.1111/(ISSN)1365-2486

Macinnis-Ng, C. M. O., Fuentes, S., O'Grady, A. P., Palmer, A. R., Taylor, D., Whitley, R. J., & Eamus, D. (2010). Root biomass distribution and soil properties of an open woodland on a duplex soil. *Plant and Soil*, *327*, 377–388. https://doi.org/10.1007/s11104-009-0061-7

Macinnis-Ng, C., Zeppel, M., Williams, M., & Eamus, D. (2011). Applying a SPA model to examine the impact of climate change on GPP of open woodlands and the potential for woody thickening. *Ecohydrology*, *4*, 379–393. https://doi.org/10.1002/eco.138

Marshall, D. C. (1958). Measurement of sap flow in conifers by heat transport. *Plant Physiology*, *33*, 385–396. https://doi.org/10.1104/pp.33.6.385

McCarthy, H. R., Oren, R., Finzi, A. C., Ellsworth, D. S., Kim, H. S., Johnsen, K. H., & Millar, B. (2007). Temporal dynamics and spatial variability in the enhancement of canopy leaf area under elevated atmospheric CO_2. *Global Change Biology*, *13*, 2479–2497. https://doi.org/10.1111/j.1365-2486.2007.01455.x

Morgan, J. A., Pataki, D. E., Körner, C., Clark, H., Del Grosso, S. J., Grünzweig, J. M., & Nippert, J. B. (2004). Water relations in grassland and desert ecosystems exposed to elevated atmospheric CO_2. *Oecologia*, *140*, 11–25. https://doi.org/10.1007/s00442-004-1550-2

Nelson, J. A., Morgan, J. A., Lecain, D. R., Mosier, A., Milchunas, D. G., & Parton, B. A. (2004). Elevated CO_2 increases soil moisture and enhances plant water relations in a long-term field study in semi-arid shortgrass steppe of Colorado. *Plant and Soil*, *259*, 169–179. https://doi.org/10.1023/B:PLSO.0000020957.83641.62

Nolan, R. H., Lane, P. N. J., Benyon, R. G., Bradstock, R. A., & Mitchell, P. J. (2014). Changes in evapotranspiration following wildfire in resprouting eucalypt forests. *Ecohydrology*, *7*, 1363–1377.

Norby, R. J., DeLucia, E. H., Gielen, B., Calfapietra, C., Giardina, C. P., King, J. S., & De Angelis, P. (2005). Forest response to elevated CO_2 is conserved across a broad range of productivity. *Proceedings of the National Academy of Sciences of the United States of America*, *102*, 18052–18056. https://doi.org/10.1073/pnas.0509478102

Nowak, R. S., Zitzer, S. F., Babcock, D., Smith-Longozo, V., Charlet, T. N., Coleman, J. S., & Smith, S. D. (2004). Elevated atmospheric CO_2 does not conserve soil water in the Mojave desert. *Ecology*, *85*, 93–99. https://doi.org/10.1890/03-3054

Oren, R., Phillips, N., Katul, G., Ewers, B. E., & Pataki, D. E. (1998). Scaling xylem sap flux and soil water balance and calculating variance: A method for partitioning water flux in forests. *Annals of Forest Science*, *55*, 191–216. https://doi.org/10.1051/forest:19980112

Paschalis, A., Katul, G. G., Fatichi, S., Palmroth, S., & Way, D. (2017). On the variability of the ecosystem response to elevated atmospheric CO_2 across spatial and temporal scales at the Duke Forest FACE experiment. *Agricultural and Forest Meteorology*, *232*, 367–383. https://doi.org/10.1016/j.agrformet.2016.09.003

Pathare, V. S., Crous, K. Y., Cooke, J., Creek, D., Ghannoum, O., & Ellsworth, D. S. (2017). Water availability affects seasonal CO_2-induced photosynthetic enhancement in herbaceous species in a periodically dry woodland. *Global Change Biology*, *23*, 5164–5178. https://doi.org/10.1111/gcb.13778

Pfautsch, S., Macfarlane, C., Ebdon, N., & Meder, R. (2012). Assessing sapwood depth and wood properties in *Eucalyptus* and *Corymbia* spp. using visual methods and near infrared spectroscopy (NIR). *Trees-Structure and Function*, *26*, 963–974. https://doi.org/10.1007/s00468-011-0674-3

Porporato, A., Daly, E., & Rodríguez-Iturbe, I. (2004). Soil water balance and ecosystem response to climate change. *American Naturlalist*, *164*, 625–632. https://doi.org/10.1086/424970

R Development Core Team (2014) R: A Language and Environment for Statistical Computing.

Raz-Yaseef, N., Rotenberg, E., & Yakir, D. (2010). Effects of spatial variations in soil evaporation caused by tree shading on water flux partitioning in a semi-arid pine forest. *Agricultural and Forest Meteorology*, *150*, 454–462. https://doi.org/10.1016/j.agrformet.2010.01.010

Raz-Yaseef, N., Yakir, D., Schiller, G., & Cohen, S. (2012). Dynamics of evapotranspiration partitioning in a semi-arid forest as affected by temporal rainfall patterns. *Agricultural and Forest Meteorology*, *157*, 77–85. https://doi.org/10.1016/j.agrformet.2012.01.015

Schäfer, K. V. R., Oren, R., Lai, C. T., & Katul, G. G. (2002). Hydrologic balance in an intact temperate forest ecosystem under ambient and elevated atmospheric CO_2 concentration. *Global Change Biology*, *8*, 895–911. https://doi.org/10.1046/j.1365-2486.2002.00513.x

Schreiner-Mcgraw, A. P., Vivoni, E. R., Mascaro, G., & Franz, T. E. (2016). Closing the water balance with cosmic-ray soil moisture measurements and assessing their relation to evapotranspiration in two semi-arid watersheds. *Hydrology and Earth System Sciences*, *20*, 329–345. https://doi.org/10.5194/hess-20-329-2016

Soubie, R., Heinesch, B., Granier, A., Aubinet, M., & Vincke, C. (2016). Evapotranspiration assessment of a mixed temperate forest by four methods: Eddy covariance, soil water budget, analytical and model. *Agricultural and Forest Meteorology*, *228*, 191–204. https://doi.org/10.1016/j.agrformet.2016.07.001

Swanson, R. H., & Whitfield, D. W. A. (1981). A numerical analysis of heat pulse velocity theory and practice. *Journal of Experimental Botany*, *32*, 221–239. https://doi.org/10.1093/jxb/32.1.221

Tor-ngern, P., Oren, R., Ward, E. J., Palmroth, S., McCarthy, H. R., & Domec, J. C. (2015). Increases in atmospheric CO_2 have little influence on transpiration of a temperate forest canopy. *New Phytologist*, *205*, 518–525. https://doi.org/10.1111/nph.13148

Trancoso, R., Larsen, J. R., McVicar, T. R., Phinn, S. R., & Mcalpine, C. A. (2017). CO_2-vegetation feedbacks and other climate changes implicated in reducing base flow. *Geophysical Research Letters*, *44*, 2310–2318.

Uddling, J., Teclaw, R. M., Pregitzer, K. S., & Ellsworth, D. S. (2009). Leaf and canopy conductance in aspen and aspen-birch forests under free-air enrichment of carbon dioxide and ozone. *Tree Physiology*, *29*, 1367–1380. https://doi.org/10.1093/treephys/tpp070

Ukkola, A. M., Prentice, I. C., Keenan, T. F., Van Dijk, A. I. J. M., Viney, N. R., Myneni, R. B., & Bi, J. (2016). Reduced streamflow in water-stressed climates consistent with CO_2 effects on vegetation. *Nature Climate Change*, *6*, 75–78. https://doi.org/10.1038/nclimate2831

Ward, E. J., Oren, R., Bell, D. M., Clark, J. S., McCarthy, H. R., Kim, H. S., & Domec, J. C. (2013). The effects of elevated CO_2 and nitrogen fertilization on stomatal conductance estimated from 11 years of scaled sap flux measurements at Duke FACE. *Tree Physiology*, *33*, 135–151. https://doi.org/10.1093/treephys/tps118

Warren, J. M., Pötzelsberger, E., Wullschleger, S. D., Thornton, P. E., Hasenauer, H., & Norby, R. J. (2011). Ecohydrologic impact of

reduced stomatal conductance in forests exposed to elevated CO_2. *Ecohydrology*, *4*, 196–210. https://doi.org/10.1002/eco.173

Wood, S. (2006). *Generalized additive models: An introduction with R*. Boca Raton, FL: CRC Press, Taylor & Francis. 397 pp.

Wullschleger, S. D., & Norby, R. J. (2001). Sap velocity and canopy transpiration in a sweetgum stand exposed to free-air CO_2 enrichment (FACE). *New Phytologist*, *150*, 489–498. https://doi.org/10.1046/j.1469-8137.2001.00094.x

Yang, Y., Donohue, R. J., & McVicar, T. R. (2016). Global estimation of effective plant rooting depth: Implications for hydrological modeling. *Water Resources Research*, *52*, 8260–8276. https://doi.org/10.1002/2016WR019392

Yang, Y. T., Donohue, R. J., McVicar, T. R., Roderick, M. L., & Beck, H. E. (2016). Long-term CO_2 fertilization increases vegetation productivity and has little effect on hydrological partitioning in tropical rainforests. *Journal of Geophysical Research-Biogeosciences*, *121*, 2125–2140. https://doi.org/10.1002/2016JG003475

Zhang, L., Dawes, W. R., & Walker, G. R. (2001). Response of mean annual evapotranspiration to vegetation changes at catchment scale. *Water Resources Research*, *37*, 701–708. https://doi.org/10.1029/2000WR900325

Zhang, Y., Peña-Arancibia, J. L., McVicar, T. R., Chiew, F. H., Vaze, J., Liu, C., & Miralles, D. G. (2016). Multi-decadal trends in global terrestrial evapotranspiration and its components. *Scientific Reports*, *6*, 19124. https://doi.org/10.1038/srep19124

Zhu, Z., Piao, S., Myneni, R. B., Huang, M., Zeng, Z., Canadell, J. G., & Cao, C. (2016). Greening of the Earth and its drivers. *Nature Climate Change*, *6*, 791–795. https://doi.org/10.1038/nclimate3004

SUPPORTING INFORMATION

Additional Supporting Information may be found online in the supporting information tab for this article.

How to cite this article: Gimeno TE, McVicar TR, O'Grady AP, Tissue DT, Ellsworth DS. Elevated CO_2 did not affect the hydrological balance of a mature native *Eucalyptus* woodland. *Glob Change Biol*. 2018;00:1–15. https://doi.org/10.1111/gcb.14139